

Article

The Recovery of TiO₂ from Ilmenite Ore by Ammonium Sulfate Roasting–Leaching Process

Mahmoud S. Abdelgalil ^{1,2} , K. El-Barawy ², Yang Ge ¹ and Longgong Xia ^{1,*} 

¹ Complex Material Metallurgy and Slag Chemistry Research Group, School of Metallurgy and Environment, Central South University, Changsha 410083, China; msoly701@gmail.com (M.S.A.); geyang@csu.edu.cn (Y.G.)

² Pyrometallurgical Processing of Ores Department, Central Metallurgical Research and Development Institute (CMRDI), P.O. Box 87, Helwan 11722, Egypt; kamilia48@hotmail.com

* Correspondence: longgong.xia@csu.edu.cn

Abstract: TiO₂ production is a key part of Ti metallurgy and Ti recycling, and the process itself has turned out to be energy-consuming and material-consuming. New technologies are needed to utilize complex Ti ores, such as ilmenite, and reduce the carbon footprint of TiO₂ extraction. Ammonium sulfate roasting has been revealed as an efficient way to carry out phase transformations of complex minerals. A low-temperature sulfation roasting approach was studied to chemically breaking down the crystal structure of ilmenite and generate metal soluble sulfates simultaneously. These roasted products were introduced to water leaching, then the residue of the water leaching was leached by diluted HCl acid, and the TiO₂ product was enriched in the leaching residue. The effects of roasting temperature, roasting time, ilmenite-to-ammonium sulfate mass ratio, ilmenite particle size, and second-stage roasting on iron removal and titanium loss leaching efficiency were systematically studied. The results show that the optimum roasting conditions were a roasting temperature of 500 °C, a roasting time of 210 min, an ilmenite-to-(NH₄)₂SO₄ mass ratio of 1:7, and an ilmenite particle size of below 43 μm. Under optimized conditions, the TiO₂ grade in the obtained synthetic rutile reached 75.83 wt.%. Furthermore, the phase transformation and reaction mechanism during roasting are discussed and interpreted.

Keywords: ammonium sulfate roasting; ilmenite ore; water leaching; phase transformation; reaction mechanism



Citation: Abdelgalil, M.S.; El-Barawy, K.; Ge, Y.; Xia, L. The Recovery of TiO₂ from Ilmenite Ore by Ammonium Sulfate Roasting–Leaching Process. *Processes* **2023**, *11*, 2570. <https://doi.org/10.3390/pr11092570>

Academic Editors: Fiseha Tesfaye and Leitong Shen

Received: 3 August 2023

Revised: 17 August 2023

Accepted: 23 August 2023

Published: 28 August 2023



Copyright: © 2023 by the authors. Licensee MDPI, Basel, Switzerland. This article is an open access article distributed under the terms and conditions of the Creative Commons Attribution (CC BY) license (<https://creativecommons.org/licenses/by/4.0/>).

1. Introduction

Titanium dioxide (TiO₂) is one of the most important white pigments, and is widely used in plastics, rubber, paints, paper, food, cosmetics, medicine, ceramics, and textile industries [1–3]. It has high potential in high-technology applications such as semiconductors, biomedical devices, and catalysts [4,5]. TiO₂ is the primary source for manufacturing Ti metal and Ti chemicals, which are used in aerospace and military applications [6]. Titanium dioxide is originally found in three crystalline forms: rutile, anatase, and brookite. The three crystals are basically pure titanium dioxide but contain slight amounts of impurities like iron, which gives it a black color [7]. TiO₂ pigment is non-toxic and offers the highest opacity, brightness, and whiteness, so it excels in the industry as a white pigment. When the titanium dioxide particle size is reduced to less than 100 nm, unfamiliar optical properties appear. This is due to its high UV absorption and high visibility in visible light [8]. Other significant features of TiO₂ pigments are their high thermal stability, superior resistance to chemical attack, and resistance to ultraviolet degradation. According to the United States Geological Survey (USGS) statistics of 2023, titanium pigment and sponge production worldwide were 9.4 and 0.35 million tons, respectively [9]. China was the largest producer of titanium pigment and sponge, estimated at 5 and 0.18 million tons, respectively [9]. Therefore, prices of TiO₂ pigment are predicted to increase in the next few years due to

the rising costs of chlorine, caustic soda, coke, and energy. Additionally, progress in the aerospace and defense industries will definitely increase titanium metal demand.

Titanium dioxide is mainly produced from rutile and ilmenite. Rutile is considered the most titanium-rich mineral, and it is used directly as a raw material for TiO_2 [10]. On the other hand, ilmenite is the most abundant titanium mineral in nature. Deposits exist on coastal beaches as sand placers and in mines as igneous rocks. Although the total world resources of ilmenite, anatase, and rutile were estimated at more than 2 billion tons [9], natural rutile reserves are limited in the earth's crust. They only represent one-tenth of ilmenite reserves [9,11]. The lack of natural rutile has led to research into the conversion of ilmenite into synthetic rutile [12,13]. There is no doubt that ilmenite will continue to dominate the titanium industry in the future as the most important titanium resource.

Ilmenite industrial practice falls into three types: smelting, chloride, and sulphate processes. These processes differ in their raw material requirements and chemistry [14]. In the smelting process [15], ilmenite is upgraded by a carbothermic process, yielding TiO_2 -rich slag as the primary product and pig iron as a by-product. More than 65% of ilmenite is smelted using electric furnaces worldwide and 85% in China, where it is the primary production method for ilmenite [16]. But the smelting process produces large amounts of CO_2 gas, which pollutes the environment and requires excessive energy consumption. Berkovich developed the chloride process to dissolve at least 80% of the titanium and iron in ilmenite ore through direct leaching with concentrated hydrochloric acid [17–19]. This method has a long process flow, low product quality, poor recovery, and high cost and waste emissions. The sulphate process was the first commercial process for producing titanium pigment from ilmenite. In this process [20,21], sulfuric acid is combined with ilmenite (40–60% TiO_2) or high-titania slag (72–87% TiO_2) in digestion to form intermediate products (titanyl sulfate and iron sulfate). The biggest challenge to developing titanium dioxide using the sulfuric acid process is waste emissions, including acid hydrolysis residue, waste acid, and acid waste water. Therefore, introducing environmentally clean technologies is necessary. In addition, there are commercialized or proposed processes to produce TiO_2 pigments from ilmenite, such as the Murso process [22], in which fluidized beds are used for thermo-conversions. Ilmenite is pre-oxidized in a fluidized bed at 900–950 °C, and another fluidized bed is used to reduce the ferric ions in the hot oxidized ore with a reducing agent like H_2 gas. Then, the product from the second fluidized bed is digested with about 20% HCl at a temperature range of 108–110 °C. In this process, it is easier to recycle HCl than in the sulfate process. In the Laporte process [23], the ore undergoes pre-oxidation in a fluidized bed at 950 °C, and it is followed by reductive roasting using coke in a rotary kiln at about 900 °C. Using coal as a reductant, ferrous oxide is formed from the ferric content in ilmenite. The roasted ore is leached with 18% HCl at atmospheric pressure for 3.5 h to eliminate the iron content, yielding synthetic rutile with high-purity TiO_2 . The Kataoka process in Japan [24] consists of trivalent iron content of ilmenite ore being reduced to ferrous oxide by reduction roasting, then leaching by sulfuric acid. The rate of precipitation of titanium salts is increased by adding hydrated TiO_2 as seeds to the leaching solution in order to improve the removal of iron species and accelerate the sedimentation of titanium salts. As a result, the Kataoka process is able to separate iron from ilmenite at lower temperatures and using less sulfuric acid, thus making it more sustainable and economically viable. TiO_2 recovery reaches more than 95%. In the Austpac process [25], ilmenite is roasted at temperatures between 800 and 1000 °C. Magnetic separation can remove gangue minerals. HCl (25%) removes iron and impurities by leaching. The produced residue is filtered, washed, and calcined. Magnetic separation is used to obtain synthetic rutile > 97% TiO_2 . The Benelite process [26] utilizes carbon thermo-reduction for converting other iron forms to ferrous states via leaching with 18–20% HCl.

Nowadays, sulfation roasting has been widely used in the metallurgical processing of complex minerals. The principle of sulfation roasting involves converting metal oxides in complex minerals into metal sulfate salts. These salts can then undergo a leaching process to produce the valuable metals [27]. Sulfuric acid can be used in sulfation roasting, but

the sulfuric acid mass fraction is high. This leads to significant corrosion of the equipment used [28]. Roasting using ammonium sulfate is similar to sulfuric acid roasting; however, sulfation roasting with ammonium sulfate is not as corrosive to the equipment. The NH_3 gas produced during the sulfation process can be recycled as ammonium sulfate again [29]. Moreover, ammonium sulfate decomposes at a lower temperature ($250\text{ }^\circ\text{C}$), which is considered an advantage from an energy requirement standpoint [30]. Several years ago, some studies investigated the extraction of metals from different minerals by using the ammonium sulfate roasting method. These minerals included vanadium slag [31], bauxite ore [32], spent lithium-ion batteries [33], manganese ore [34], and nickel sulfide ores [35]. Some studies have been conducted on ilmenite ore using ammonium sulfate roasting. Malaysian ilmenite was roasted using ammonium sulfate in an N_2 atmosphere. The separation process was performed by adjusting the pH of the solution and adding rutile as well as iron scrap seeds [36]. However, the flowsheet was long and the reaction mechanism was not involved in the roasting process. Panzhihua ilmenite was roasted using ammonium sulfate in an N_2 atmosphere in two steps: The first step was the sulfation of ilmenite at a lower temperature, and in the second step, the optimum sulfated sample was thermally decomposed at a higher temperature [37]. However, the study focused on the factors that affect the leaching process, with little consideration given to the parameters that affect roasting.

Hereby, the present work proposes a route for TiO_2 recovery from ilmenite ore via an ammonium sulfate roasting process. This is to achieve the mineral phase transformation of metal oxides to soluble metal sulfate salts. The obtained roasted product is leached with distilled water and acid leaching followed by calcination to produce synthetic rutile. This proposal focuses on enhanced selective TiO_2 recovery and maximized leaching efficiency of iron from roasted ilmenite. The effects of roasting factors including roasting temperature, roasting time, mass ratio of ilmenite to ammonium sulfate, and ilmenite particle size on the leaching efficiency of iron removal and titanium loss are investigated in detail. Previous articles have demonstrated that the complexity of the chemical structure of ilmenite ore prevents selective TiO_2 recovery and increases energy requirements. Therefore, in this study, the reaction mechanism of the roasting process is discussed in depth. It has been reported that few studies have investigated the effect of ilmenite particle size on leaching efficiency during roasting. Additionally, the effect of second-stage roasting on leaching efficiency is investigated. Therefore, the study aims to cover all of these factors that have not been reported previously. The process is simple, short, easy to implement, and environmentally friendly.

2. Materials and Methods

2.1. Materials

A black sand ilmenite ore was received from the Nuclear Materials Authority in Egypt. The chemical composition, phase composition, and morphology of the ore are presented in Table 1 and Figure 1.

Table 1. Chemical composition of the black sand ilmenite ore (wt.%).

Component	TiO_2	Total Fe	SiO_2	CaO	MnO	MgO	Al_2O_3	V_2O_5
Content wt. %	43.13	36.45	2.35	1.55	1.16	1.16	0.81	0.32

The X-ray diffraction (XRD) analysis of the ilmenite is shown in Figure 1a, which indicates that the major mineral phases are FeTiO_3 and Fe_2O_3 . Figure 1b indicates the morphology of the raw material of the ilmenite ore supported by energy dispersive spectroscopy (EDS) analysis. The main components are two different grains; the light grain is the FeTiO_3 phase with a complex crystal structure between iron and titanium oxides. The other light grain with dark shades from SiO_2 and metal silicate impurities in Figure 1c was observed at high magnification. The chemical composition of the ilmenite ore was deter-

mined by inductively coupled plasma optical emission spectrometry (ICP-OES). Table 1 indicates that the main metal oxides are iron oxides with a total Fe of 36.45 wt.% and TiO_2 of 43.13 wt.%, in addition to SiO_2 of 2.35 wt.% and CaO of 1.55 wt.% as the major impurities. Other impurities include traces of Mn, Mg, Al, and V oxides. These traces form shades of metal silicates with Si. During the experiments, the $-74 \mu\text{m}$ fraction of the ore was utilized. The chemicals, including $(\text{NH}_4)_2\text{SO}_4$ and HCl acid, were analytical reagent grade purchased from Sinopharm Chemical Reagent Co. Ltd, Shanghai, China.

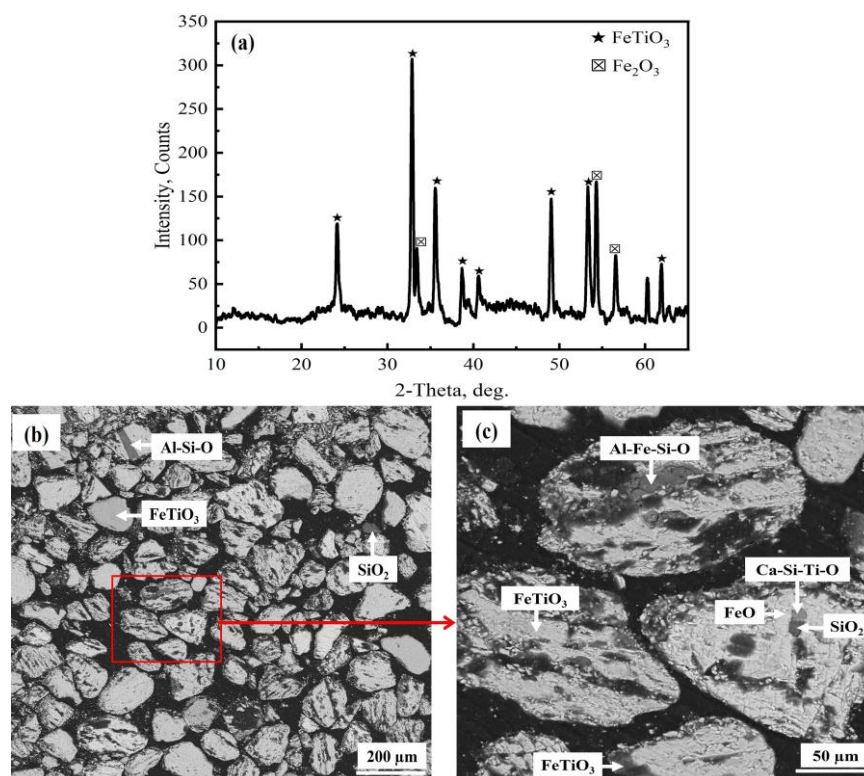


Figure 1. (a) XRD pattern of ilmenite ore, (b) SEM-EDS analysis of ilmenite ore at 200 μm , (c) SEM-EDS analysis of ilmenite ore at 50 μm .

2.2. Methods

The ilmenite ore was dried for 6 h in a drying oven. The dried sample of 3 ± 0.005 g of ilmenite was mixed with ammonium sulfate in an agate mortar to obtain a homogeneously mixed powder. The sample was placed in an alumina crucible for each roasting experiment, as shown in Figure 2.

The crucible with the sample was pushed into the hot zone in a horizontal electric tube furnace (SG-GL1200, Shanghai Institute of Optics and Fine Mechanics, Chinese Academy of Science, Shanghai, China), and a vacuum pump was used to remove the air from the quartz tube by inserting argon gas for 20 min before switching on the furnace to heat it up to the required temperature. The heating rate was $8 \text{ }^\circ\text{C}/\text{min}$, and the argon gas flow rate was maintained at 50 mL/min via a flow controller. The sample was left in the hot zone for roasting at the target temperature. As soon as the roasting experiment was completed, the crucible was slowly pulled out to the cool zone using metallic wire, in the presence of argon flow gas, in order to cool it quickly. Some parameters that could have influenced the roasting experiment were investigated, such as roasting temperature (350–600 $^\circ\text{C}$), roasting time (60–240 min), mass ratio of ilmenite ore to ammonium sulfate (1:3 to 1:11), and ilmenite particle size.

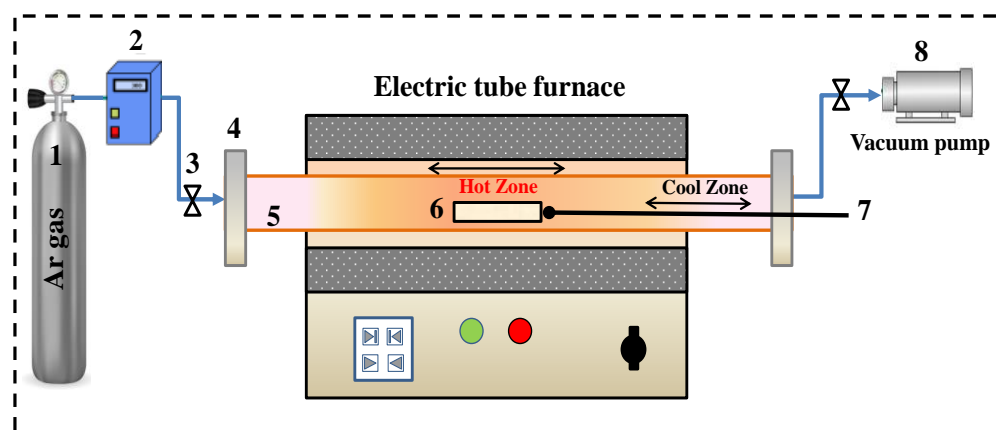


Figure 2. Horizontal electric tube furnace for roasting: (1) argon gas tube; (2) mass flow controller; (3) valve; (4) steel flange; (5) quartz tube; (6) crucible with sample; (7) metallic wire; (8) vacuum pump.

The roasted product was weighed in each experiment to determine the relative weight loss, and a sample of 4 ± 0.005 g was leached after grinding it with distilled water in a water bath (leaching temperature = 50 °C, liquid–solid ratio = 10 mL/g, magnetic stirring speed = 150 rpm, leaching time = 1 h). After water leaching, the solid residue from the water leaching was leached using a diluted HCl acid solution of 2.5 wt.% (leaching temperature = 98 °C, liquid–solid ratio = 50 mL/g, magnetic stirring speed = 150 rpm, leaching time = 2 h). The optimum acid leaching residue was thoroughly rinsed with water and calcined at 1000 °C for 1 h to obtain synthetic rutile. The leaching efficiency is mainly used to evaluate the roasting process efficiency, and the leaching efficiency is calculated as follows:

$$\eta = \frac{c_1 \times v_1 \times 10^{-3}}{m_1 \times w_1} \times 100 \quad (1)$$

η : iron removal efficiency, titanium loss (wt.%), c_1 : Fe or Ti concentration in the solution ($\text{g} \cdot \text{L}^{-1}$), v_1 : volume in the leaching solution (mL), m_1 : mass of roasted sample (g), and w_1 : Fe or Ti mass percentage in ilmenite (wt.%).

2.3. Analytical Methods

Thermogravimetric analysis and differential scanning calorimetry (TG-DSC, NET-ZSCH, STA 449 F3, and Germany) were conducted to investigate the thermal composition behaviors of ammonium sulfate and a mixture of ilmenite and ammonium sulfate. Phase identification for the products was conducted using an X-ray powder diffractometer (XRD, Rigaku Company, Tokyo, Japan, D/max-2500) to determine their qualitative mineralogical composition, and a copper-K α anode target, a wavelength λ of 1.54 Å, a scanning range of 10° – 80° , and a scanning speed of 10° /min were employed. Elemental chemical composition of the materials and metal concentrations in the leachate were determined by inductively coupled plasma optical emission spectrometry (ICP-OES) (ICAP7400 Radial, Thermo Fisher, Waltham, MA, USA). Products from the experiments were mounted in epoxy, ground, and polished to observe their morphology using a scanning electron microscope (SEM, Tescan, Brno, Czech Republic) and energy dispersive spectroscopy (EDS, Thermo Fisher Scientific, Waltham, MA, USA).

3. Results and Discussion

3.1. Sulfation Roasting

3.1.1. Effect of Roasting Temperature

The influence of roasting temperature on the leaching efficiency of iron removal and titanium loss in the leaching solution was studied from 350 °C to 600 °C under a mass ratio of ilmenite to $(\text{NH}_4)_2\text{SO}_4$ of $1:5$, a roasting time of 120 min, and an ilmenite particle size of <74 μm . In order to evaluate the roasting process, the leaching efficiency of iron removal

is an important indicator. The roasted products obtained under different conditions were leached in water followed by diluted HCl treatment of the residue of the water leaching. In other words, the sulfation process breaks down the chemical structure of ilmenite metal oxides and converts metal oxides into soluble metal sulfates. As shown in Figure 3a, the leaching efficiency of iron and titanium loss was 10.3% and 7.1%, respectively, at an operating temperature of 350 °C. By increasing the temperature to 500 °C, iron removal and Ti loss efficiency were increased to 34.4% and 11.9%, respectively. Up to 500 °C, iron removal and Ti loss were decreased to 18.8% and 0.8%, respectively. This decrease is due to the decomposition of metal sulfate or ammonium metal sulfate salts into oxides at higher temperatures.

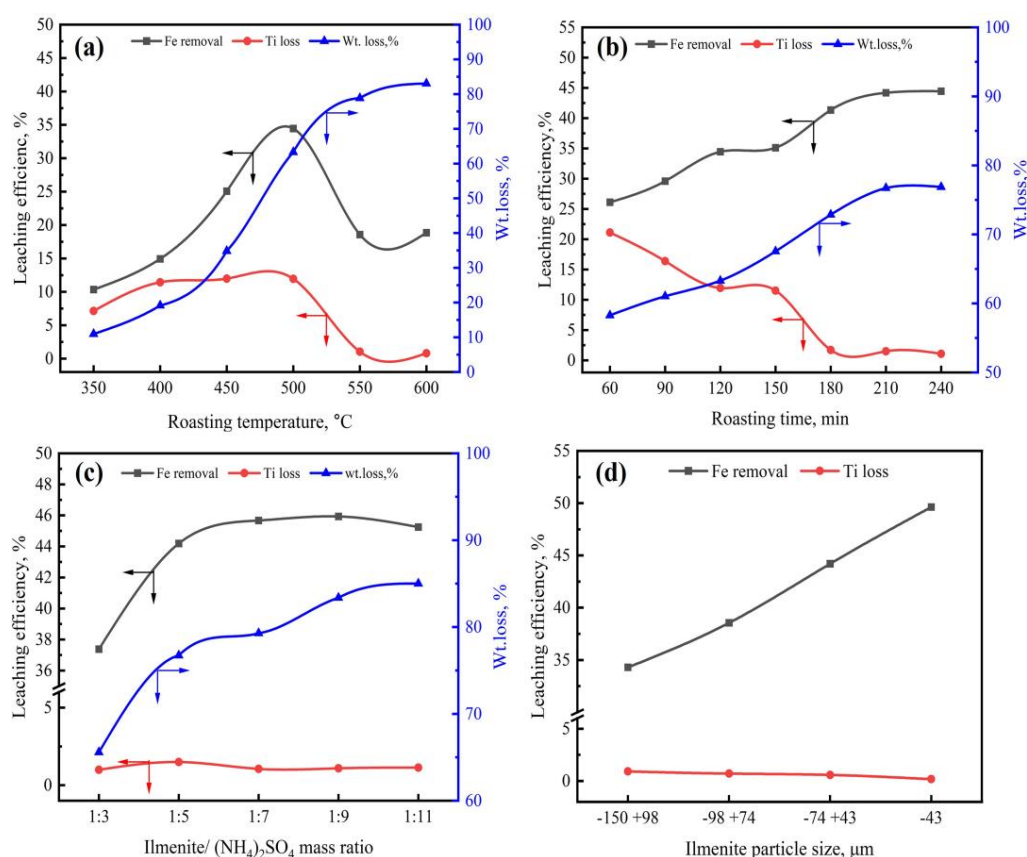


Figure 3. (a) Effect of roasting temperature on the leaching efficiency at roasting conditions (ilmenite to $(\text{NH}_4)_2\text{SO}_4$ mass ratio of 1:5, roasting time of 120 min). (b) Effect of roasting time on the leaching efficiency at roasting conditions (ilmenite to $(\text{NH}_4)_2\text{SO}_4$ mass ratio of 1:5, 500 °C). (c) Effect of ilmenite to $(\text{NH}_4)_2\text{SO}_4$ mass ratio on the leaching efficiency at roasting conditions (500 °C, 210 min). (d) Effect of ilmenite particle size on the leaching efficiency at roasting conditions (500 °C, 1:7 mass ratio, 210 min).

Figure 4a shows the color change of roasted products after they are roasted. It is shown that the roasted product was still black at 350 °C, which can be attributed to the sulfation process in the beginning stage. The color of the roasted product became whitish with increasing temperature. At higher temperatures up to 550 °C, the color became brown. The color change of the roasted products agreed well with the weight loss curve after roasting at different temperatures. This is shown in Figure 3a, where the weight loss at 600 °C reached 83%. It is not recommended to roast at higher temperatures because the metal sulfate salts or ammonium metal sulfate will decompose into their respective oxides during roasting.

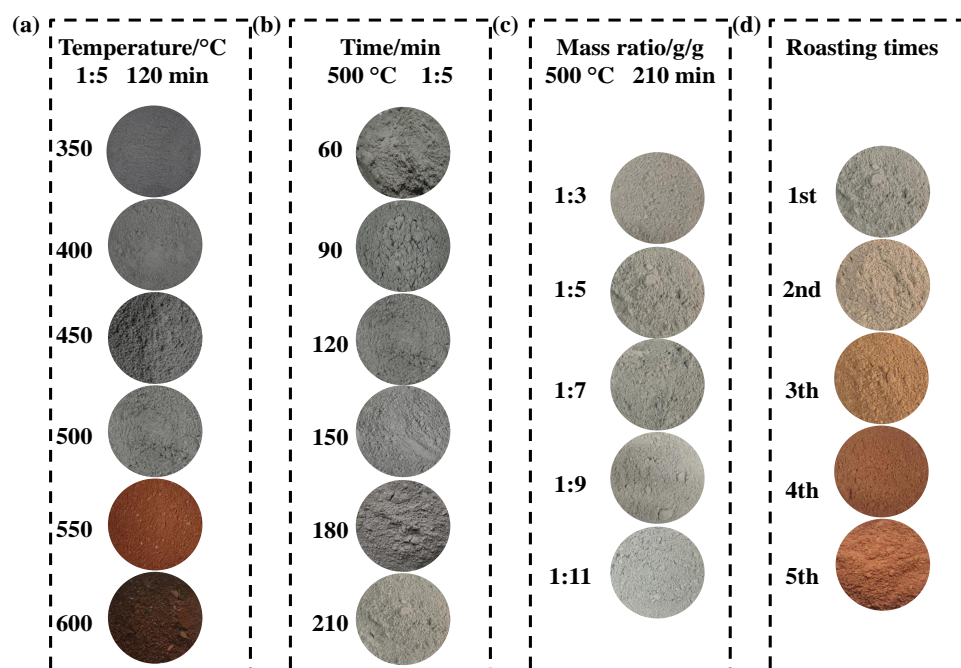


Figure 4. Digital pictures of roasted products obtained under different conditions of (a) roasting temperature, (b) roasting time, (c) ilmenite-to-ammonium sulfate mass ratio, and (d) No. of roasting times.

The XRD pattern of roasted products at roasting temperatures ranging from 350 °C to 550 °C is shown in Figure 5. It is clear from the roasting process that the temperature significantly affected conversion. At a roasting temperature of 350 °C, the $(\text{NH}_4)_3\text{H}(\text{SO}_4)_2$ phase appeared due to ammonium sulfate decomposition. In addition, some peaks of the $(\text{NH}_4)_3\text{Fe}(\text{SO}_4)_3$ phase formed due to the reaction of $(\text{NH}_4)_3\text{H}(\text{SO}_4)_2$ with ilmenite ore. Additionally, diffraction peaks of $(\text{NH}_4)_2\text{SO}_4$ were observed, which indicates that the decomposition was not completed. At a roasting temperature of 400 °C, all of the $(\text{NH}_4)_2\text{SO}_4$ decomposed into the $(\text{NH}_4)_3\text{H}(\text{SO}_4)_2$ phase, which reacted directly with ilmenite to produce $(\text{NH}_4)_3\text{Fe}(\text{SO}_4)_3$ and $\text{FeSO}_4 \cdot 4\text{H}_2\text{O}$. When the temperature was increased to 450 °C, the diffraction peaks of the $(\text{NH}_4)_3\text{H}(\text{SO}_4)_2$ phase completely disappeared, indicating that all amounts of $(\text{NH}_4)_3\text{H}(\text{SO}_4)_2$ reacted with the ilmenite ore. The main phase was $\text{NH}_4\text{Fe}(\text{SO}_4)_2$, which was directly converted from of the $(\text{NH}_4)_3\text{Fe}(\text{SO}_4)_3$ phase. By increasing the temperature to 500 °C, $\text{Fe}_2(\text{SO}_4)_3$, TiOSO_4 , and traces of Fe_2O_3 phases appeared and the peak intensity of $\text{NH}_4\text{Fe}(\text{SO}_4)_2$ decreased. By increasing the temperature to 500 °C, TiO_2 and Fe_2O_3 appeared due to the transformation of ammonium metal sulfates and metal sulfates salts into their respective oxides. This study converted the metal oxides in the ore to ammonium metal sulfate and metal sulfates because these compounds easily dissolve in water. In order to save energy and guarantee high leaching efficiency, the roasting temperature of 500 °C was selected as an optimal operating temperature for studying the other factors.

The morphology of the products after roasting at different temperatures was examined by SEM-EDS analysis. Figure 6a shows that the product roasted at 400 °C obtained surface roughness, which could have resulted from the excess of produced gases, indicating that the roasting reaction had begun, which is in good agreement with the XRD results at 400 °C. As shown in Figure 6b, the micrograph at 500 °C showed non-uniform particle size distribution and less porosity than at 400 °C. Fe and Ti sulfate phases appeared in dark colors. At high magnification, as shown in Figure 6d, the ilmenite phase (FeTiO_3) had a very complex crystal structure due to the interaction of iron and titanium oxides in the crystal structure. It was observed that ammonium sulfate reacted with the outer surface of the ilmenite phase to form metal sulfates, which appeared in a grey color on

the outer layer of the ilmenite phase, and the FeTiO_3 phase is indicated by the white areas, which show that there were many particles of the ilmenite phase that were not sulfated yet. The micrograph at 550°C , as shown in Figure 6c, is different than the sample roasted at 500°C . This is because there were fewer residuals of ammonium sulfate, the roasted particles became smaller, and a small fusion was detected. Furthermore, the micrograph of the residue after leaching at 500°C is shown in Figure 6e. The residue had two crystalline phases, FeTiO_3 and TiO_2 , but the ilmenite phase was still found in the residue in high amounts. These findings indicate that the roasting process did not occur completely.

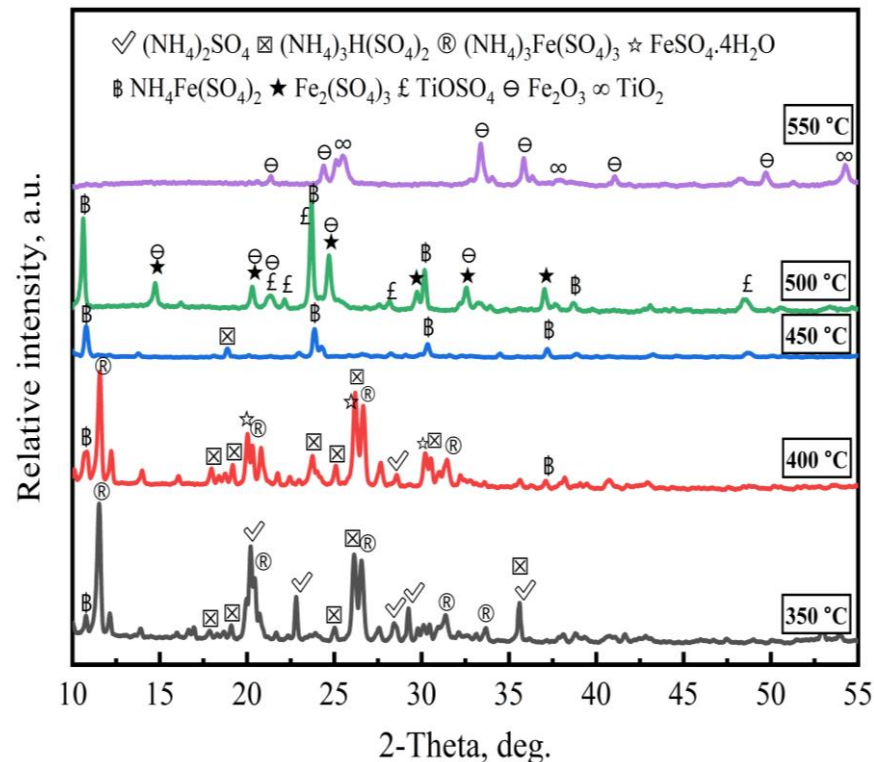
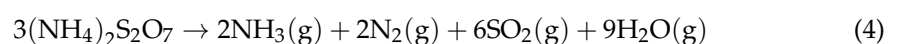
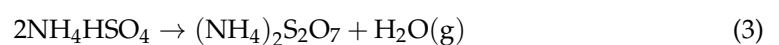


Figure 5. XRD patterns of the roasted products at different temperatures at roasting conditions (ilmenite-to- $(\text{NH}_4)_2\text{SO}_4$ mass ratio of 1:5 and roasting time of 120 min).

The thermal decomposition of pure ammonium sulfate and the mixture of ilmenite and ammonium sulfate were investigated using TG/DSC at a heating rate of $5^\circ\text{C}/\text{min}$ to 800°C in the argon atmosphere (Figure 7). As shown in Figure 7a, $(\text{NH}_4)_2\text{SO}_4$ showed better stability below 250°C , and the first stage of weight loss was 13.9% from 250 to 305.3°C , which may match the NH_3 release in Equation (2). In the second stage, a weight loss of 7.8% was observed between 305.3 and 344.8°C , which corresponds with the occurrence reaction in Equation (3) (theoretical weight loss of 6.81%). In the final stage, a big weight loss step appeared in the range of 344.8 to 413.7°C , with a weight loss of 74.09%, which agrees with the process of $(\text{NH}_4)_2\text{S}_2\text{O}_7$ decomposition into NH_3 , N_2 , SO_2 , and H_2O according to Equation (4) [38,39]. This indicates that ammonium sulfate decomposition was completed.



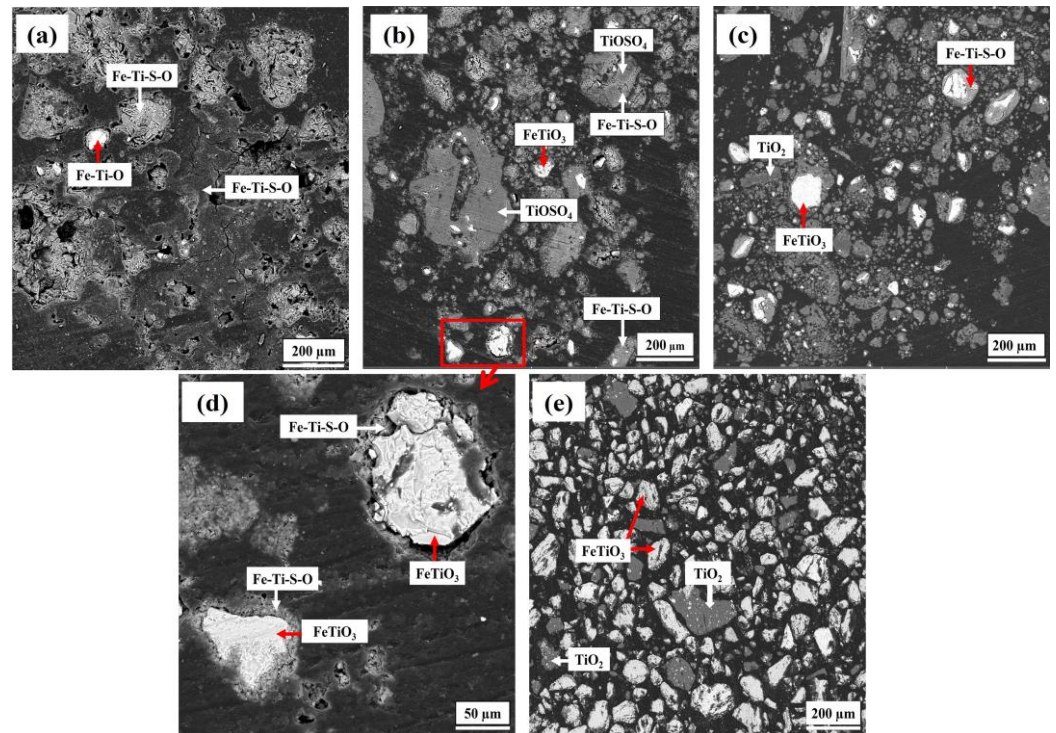


Figure 6. SEM–EDS results of the roasted products at roasting temperatures of (a) 400 °C, (b) 500 °C, (c) 550 °C, and (d) 500 °C at 50 μm, and (e) residue after acid leaching.

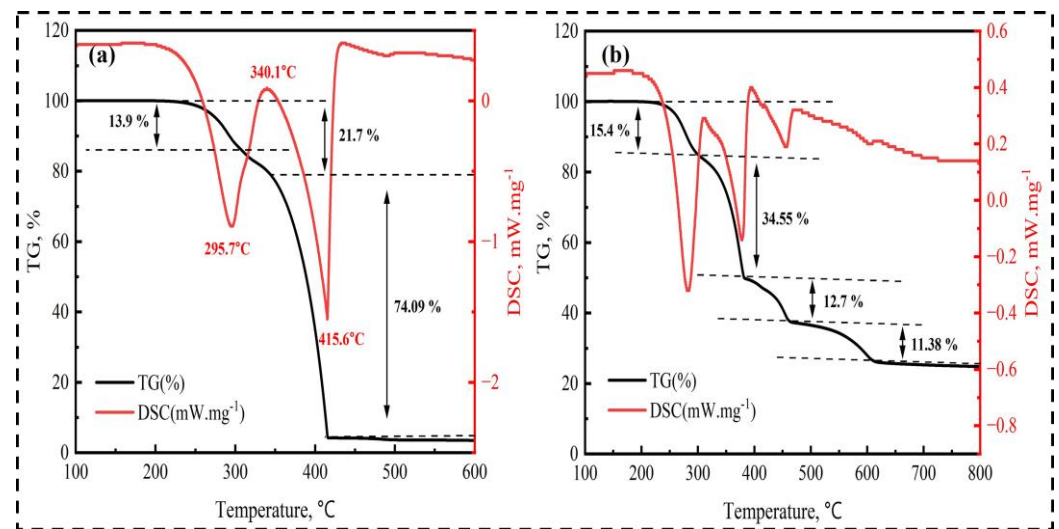
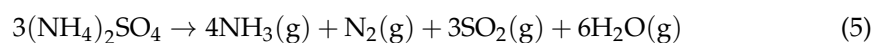


Figure 7. Simultaneous TG/DSC curves for the (a) pure ammonium sulfate and (b) mixture of ilmenite and ammonium sulfate (heating rate: 5 °C/min, argon atmosphere, ilmenite-to-ammonium sulfate mass ratio = 1:3).

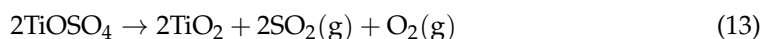
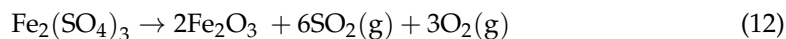
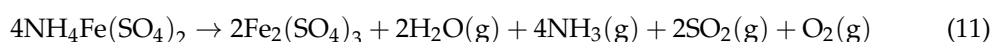
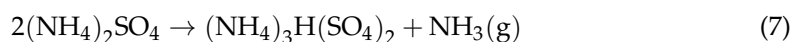
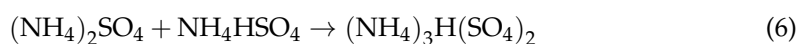
The overall reaction is:



The TG-DSC curves of the mixture of ilmenite and ammonium sulfate from 100 to 800 °C are shown in Figure 7b. The mixture property did not change below 250 °C, indicating that no reaction occurred at this stage. When the temperature rose to 300 °C, the mixture had a weight loss rate of about 15.4%. Based on the TG-DSC curves of $(\text{NH}_4)_2\text{SO}_4$ and the above analysis results, it can be concluded that $(\text{NH}_4)_2\text{SO}_4$ was decomposed into

$(\text{NH}_4)_2\text{S}_2\text{O}_7$, NH_3 , and H_2O at this stage. In addition, $(\text{NH}_4)_3\text{H}(\text{SO}_4)_2$ could have been formed according to Equations (6) and (7). When the temperature increased to $380\text{ }^\circ\text{C}$, a big weight loss step appeared, and the weight loss rate was 34.55%. This resulted from the reaction in Equations (8) and (9) between ilmenite and $(\text{NH}_4)_3\text{H}(\text{SO}_4)_2$ to generate the corresponding sulfates. As the temperature was raised to $462\text{ }^\circ\text{C}$, the mixture lost 12.7% weight as a result of the reactions listed in Equations (10) and (11), during which the ammonium metal sulfate phase transforms into the metal sulfate phase. These results agree with the XRD pattern at the same temperature. In the last stage, from 462 to $600\text{ }^\circ\text{C}$, the weight loss was about 11.38% due to the reactions listed in Equations (12) and (13), in which the metal sulfate phases transform into metal oxides. This indicates that the reaction finished at this stage.

Based on the XRD, SEM-EDS, and TGA-DSC data, the expected reaction mechanism during the roasting process was investigated at different temperatures in the following reactions [38,40,41].



3.1.2. Effect of Roasting Time

The effect of roasting time, ranging from 60 min to 240 min, on the leaching efficiency of iron and titanium loss was investigated under the mass ratio of ilmenite to $(\text{NH}_4)_2\text{SO}_4$ of 1:5, a roasting temperature of $500\text{ }^\circ\text{C}$, and an ilmenite particle size of $<74\text{ }\mu\text{m}$. Figure 3b shows that at a roasting time of 60 min, the leaching efficiency of Fe removal and Ti loss were only approximately 26.1% and 21.1%, respectively. By increasing the roasting time to 210 min, an increased leaching efficiency of iron of approximately 44.1% was reached, whereas Ti loss in the solution decreased to 1.5%. By further expanding roasting time to 210 min, the leaching efficiency of iron was still steady at 44.4% and Ti loss in the solution decreased slightly to 1%. The weight loss of the roasted products after roasting at different roasting times ranged from 58% to 77%, as shown in Figure 3b. In addition, there was a slight change in the color of the roasted products, as shown in Figure 4b, because the difference in the weight loss at different roasting times was not as large compared with the weight loss in the previous parameter.

Figure 8 shows the XRD pattern of the roasted products at roasting times ranging from 60 min to 210 min. The roasting time clearly affected the phase transformation. At 60 to 90 min of roasting time, $\text{NH}_4\text{Fe}(\text{SO}_4)_2$ was the primary phase. By increasing the roasting time from 120 to 180 min, the intensity of the diffraction peaks of $\text{NH}_4\text{Fe}(\text{SO}_4)_2$ decreased. New phases of $\text{Fe}_2(\text{SO}_4)_3$, TiOSO_4 and traces of Fe_2O_3 appeared. This means that by increasing roasting time, the ammonium iron sulfate phase transformed into ferric sulfate according to Equation (11). At a high roasting time of 210 min, the diffraction peaks of ammonium iron sulfate completely disappeared beside the existing $\text{Fe}_2(\text{SO}_4)_3$, TiO_2 , and Fe_2O_3 phases. Another FeSO_4 phase appeared, possibly due to converting some of the

$\text{Fe}_2(\text{SO}_4)_3$ into FeSO_4 . It seems that the XRD patterns of various roasting times aligned well with those of XRD patterns at different roasting temperatures.

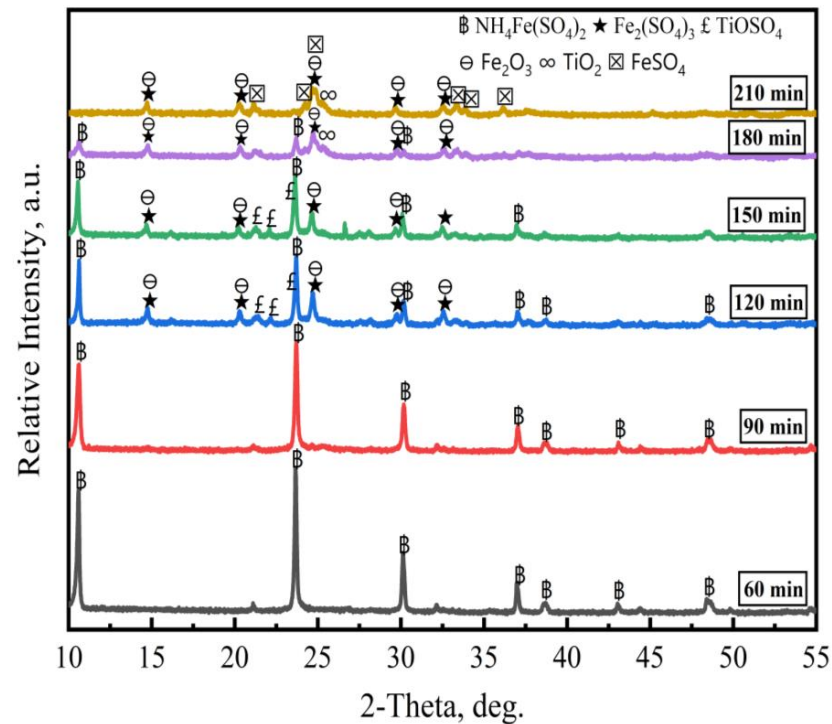


Figure 8. XRD patterns of the roasted products at various roasting times at roasting conditions (ilmenite-to- $(\text{NH}_4)_2\text{SO}_4$ mass ratio of 1:5 and roasting temperature of 500 °C).

The morphology of the roasted product and the residue of acid leaching at a roasting time of 210 min were examined by SEM-EDS analysis. Figure 9a depicts the roasted product at 210 min, showing a non-sulfated ilmenite phase surrounded by a metal sulfate-phase layer. The residue after leaching at 210 min was investigated by SEM-EDS, as shown in Figure 9b. The residue had two main crystalline phases, FeTiO_3 and TiO_2 , and the ilmenite phase was still found in the residue in smaller amounts than in Figure 6e. From the SEM-EDS images, we concluded that the non-sulfated ilmenite phases remained in the residue after leaching, which indicates that the roasting process did not occur completely. To study the next factors, 210 min was selected as the optimal roasting time.

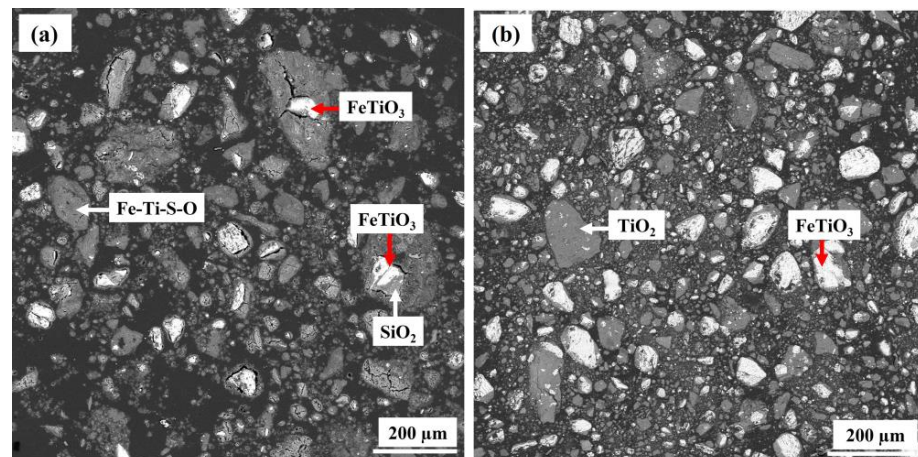


Figure 9. (a) SEM-EDS of roasted product at a roasting time of 210 min. (b) SEM-EDS of residue after acid leaching at a roasting time of 210 min.

3.1.3. Effect of Ilmenite-to-(NH₄)₂SO₄ Mass Ratio

The dosage of (NH₄)₂SO₄ required for high iron leaching is a critical factor for the roasting process. The effect of the ilmenite ore-to-(NH₄)₂SO₄ mass ratio on the leaching efficiency of iron and titanium loss was investigated under the following optimal conditions: roasting temperature of 500 °C, roasting time of 210 min, and ilmenite particle size of <74 μm. Figure 3c shows that increasing the mass ratio of ilmenite to ammonium sulfate promoted the leaching efficiency. However, increasing the ratio further may have affected the leaching efficiency. At a mass ratio of 1:3, the leaching efficiency of Fe removal and Ti loss was only approximately 37.3% and 0.9%, respectively. Increasing the mass ratio to 1:7 further enhanced the iron leaching efficiency by 45.6%, whereas Ti loss was 1%. The leaching efficiency of iron and Ti loss was still fixed at around 45.2% and 1% at a mass ratio from 1:7 to 1:11, respectively. When more (NH₄)₂SO₄ was added, a large amount of foam formed in the roasted sample. This foam was formed due to the large amounts of gas products released during roasting. Due to the difference in density between ilmenite particles and foam, the reactants were divided into two layers. In this reaction, ilmenite sunk into the lower layer, whereas ammonium bisulfate floated in the upper layer, which caused irregular mixing of the ilmenite and (NH₄)₂SO₄, leading to lower leaching efficiency. This was obvious at a mass ratio of 1:11; the weight loss of the roasted sample reached approximately 85%, as shown in Figure 3c. In addition, it was observed that the color change of the roasted samples turned whitish by increasing the ammonium sulfate dosage, as shown in Figure 4c.

The XRD pattern of the roasted samples at an ilmenite-to-(NH₄)₂SO₄ mass ratio of 1:3 to 1:11 is shown in Figure 10. At a mass ratio of 1:3, the main phases in the roasted sample were FeSO₄, Fe₂(SO₄)₃ and TiO₂. By increasing the dosage of ammonium sulfate from a mass ratio of 1:5 to 1:11, NH₄Fe(SO₄)₂ and Fe₂O₃ phases appeared. Based on these XRD patterns, the last two parameters also matched. Therefore, the mass ratio of 1:7 was chosen as an optimum operating mass ratio to study the next parameters.

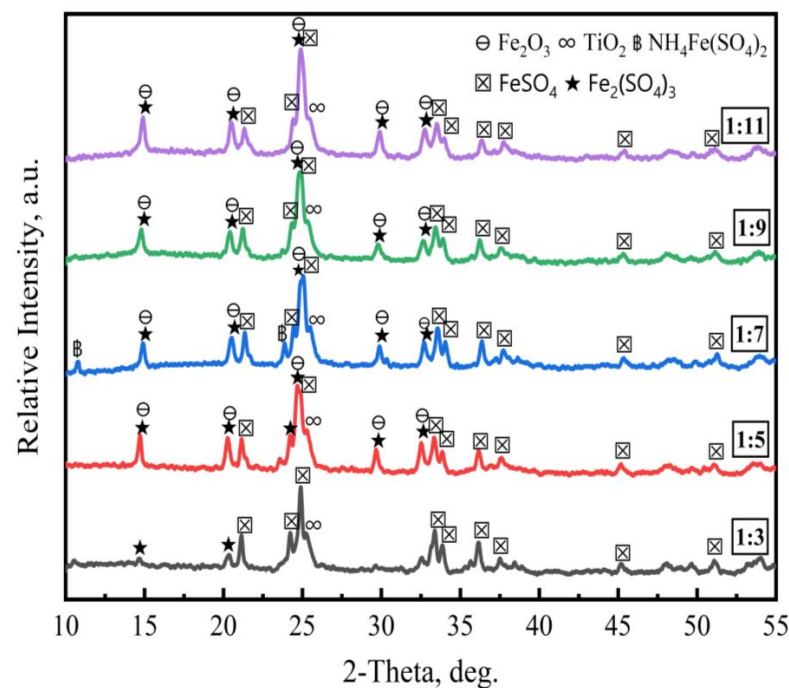


Figure 10. XRD patterns of the roasted samples at different ilmenite-to-(NH₄)₂SO₄ mass ratios at roasting conditions (roasting temperature of 500 °C and roasting time of 210 min).

3.1.4. Effect of Ilmenite Particle Size

The influence of ilmenite particle size on the leaching efficiency of iron and titanium loss was studied under the following conditions: roasting temperature of 500 °C, roast-

ing time of 210 min, and ilmenite-to- $(\text{NH}_4)_2\text{SO}_4$ mass ratio of 1:7. Figure 3d shows the relationship between iron leaching efficiency and titanium loss with ilmenite particle size. The leaching efficiency of Fe removal and Ti loss was only approximately 34.2% and 0.9%, respectively, at an ilmenite particle size of 150 to 98 μm . The leaching efficiency of Fe increased significantly with the ilmenite particle size decreasing from 150 to less than 43 μm , so the optimum leaching efficiency of iron was 49.6% at an ilmenite particle size of less than 43 μm . Furthermore, the Ti loss in the leaching solution decreased to 0.1% by reducing the ilmenite particle size. When the ilmenite particle size was finer, its crystal structure was more easily broken down and iron oxide was released more easily. Energy consumption was high when grinding the ore particles to smaller sizes, although high leaching efficiency was achieved.

3.2. Effect of Second-Stage Roasting

The effect of second-stage roasting was studied to enhance the iron removal leaching efficiency at the following roasting conditions: roasting temperature of 500 $^\circ\text{C}$, roasting time of 210 min, roasted sample-to- $(\text{NH}_4)_2\text{SO}_4$ mass ratio of 1:4, and ilmenite particle size of <43 μm . Figure 11a shows that second-stage roasting improved the iron removal efficiency, where the iron removal efficiency increased from 49.6% to 53.3%. In addition, Ti loss increased slightly to 0.3% in the leaching solution. The color change of the roasted products after roasting more than one time was clear, as shown in Figure 4d. It changed from whitish at the first stage of roasting to brown at the fourth stage of roasting. This is due to the thermal decomposition of ammonium metal sulfate and metal sulfates into metal oxides. Figure 11b shows the morphology of the roasted product after second-stage roasting, where the dark grains of Fe and Ti sulfates appear in agglomerates and the white grains are non-sulfated ilmenite.

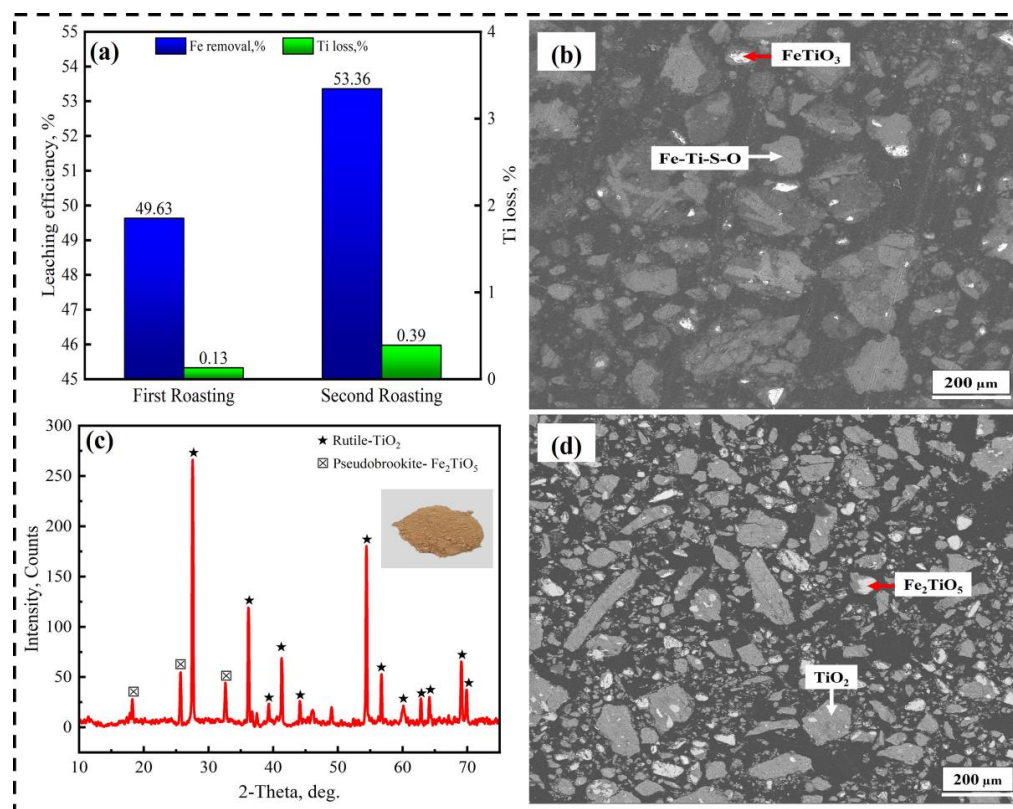


Figure 11. (a) Effect of second-stage roasting on the leaching efficiency. (b) SEM-EDS of the roasted product after second-stage roasting. (c) XRD pattern of the final product at optimum conditions after calcination. (d) SEM-EDS of the final product after calcination.

The residue of second-stage roasting after acid leaching was washed with pure water, dried, and calcined at 1000 °C for 1 h. Figure 11c shows that the main phase of the final product was rutile (TiO_2), and a small diffraction peak of pseudobrookite (Fe_2TiO_5) resulted from the oxidation of non-sulfated ilmenite in the residue during calcination. Based on Figure 11d, the morphology of the final product is consistent with the XRD analysis, which showed that the main gray phase was rutile and the small light areas were pseudobrookite. Table 2 shows the chemical composition of the final product, determined by ICP-OES, where the TiO_2 grade reached 75.83 wt.%.

Table 2. Chemical composition of synthetic rutile after calcination (wt.%).

Component	TiO_2	Total Fe	SiO_2	CaO	MnO	MgO	Al_2O_3	V_2O_5
Content wt. %	75.83	16.53	4.26	0.06	0.27	0.11	0.30	0.92

3.3. Reaction Mechanism

Figure 12 illustrates the conversion mechanism of ilmenite ore during the sulfation roasting process. Firstly, $(\text{NH}_4)_2\text{SO}_4$ gradually decomposes at temperatures greater than 250 °C to produce $(\text{NH}_4)_3\text{H}(\text{SO}_4)_2$, NH_3 , and H_2O , as shown in Equations (2), (6) and (7), respectively. The formed $(\text{NH}_4)_3\text{H}(\text{SO}_4)_2$ reacts with ilmenite ore. By increasing the roasting temperature, the metal oxides in the ore convert to $\text{NH}_4\text{Fe}(\text{SO}_4)_2$ and TiOSO_4 according to Equations (8) and (9), respectively. By increasing the roasting temperature, $\text{NH}_4\text{Fe}(\text{SO}_4)_2$ transforms to $\text{Fe}_2(\text{SO}_4)_3$ and Fe_2O_3 , but TiOSO_4 transforms to TiO_2 , as shown in Equations (10)–(13), respectively. The roasted sample is leached in water to remove water-soluble sulfate salts. The residue of the water leaching is leached by diluted HCl solution to remove some of the Fe_2O_3 formed as a result of the iron sulfate decomposition. The final product consists of TiO_2 phase and some ilmenite particles that are not sulfated during the roasting process.

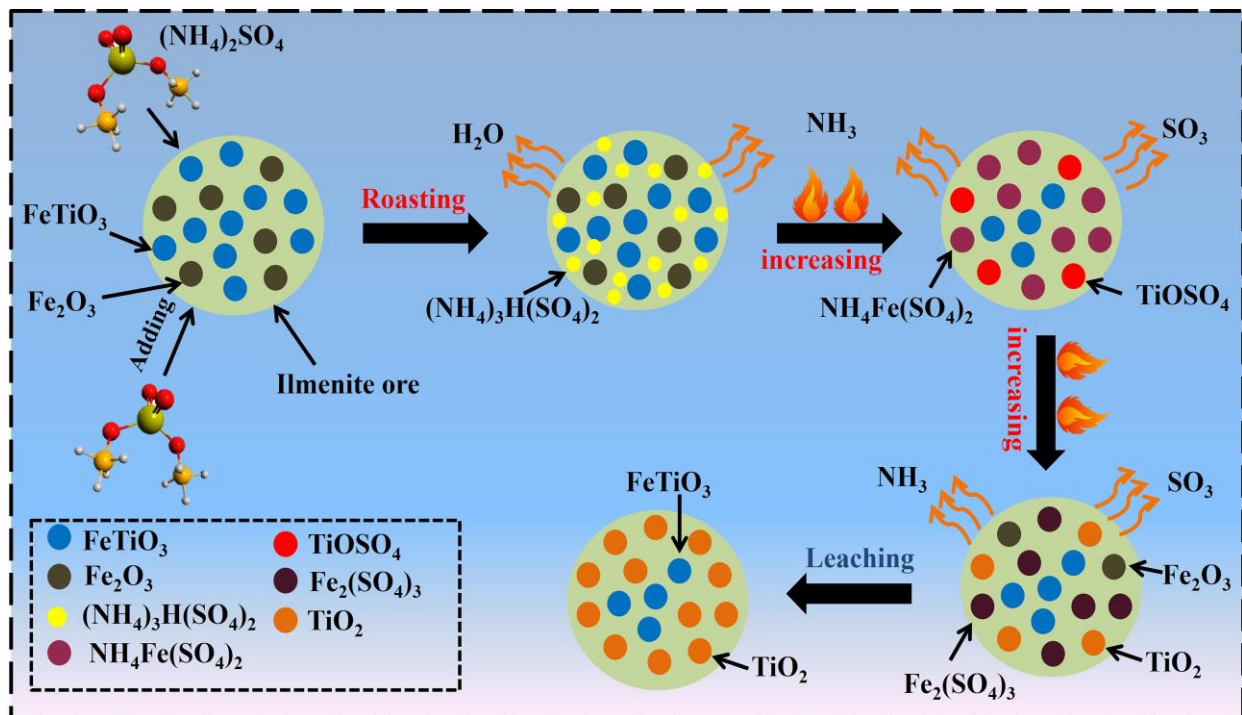


Figure 12. Schematic diagram of roasting–leaching ilmenite ore.

3.4. Flow Sheet

A proposed flow sheet with optimal conditions for recovering TiO_2 from ilmenite based on this study's results is shown in Figure 13. The ilmenite is first roasted with ammonium sulfate. The roasted sample is thus leached in water to dissolve the water-soluble sulfate. The residue of the water leaching is followed by diluted HCl to remove some of the iron oxides formed by iron sulfate decomposition during the roasting process. The residue of acid leaching at optimum conditions is calcined to obtain synthetic rutile. The NH_3 and SO_3 gases released during roasting can be efficiently absorbed by water. Then, ammonium sulfate can be acquired through evaporation and crystallization. Additionally, solution containing iron can be recycled by separating iron chloride through evaporation. Via pyrolysis, iron chloride is transformed into hydrochloric acid and iron oxide is produced. The HCl acid can be reused again, and the iron oxide can be used as a feedstock for cement production, steel production, or other purposes. This not only reduces environmental pollution but also reduces raw material consumption.

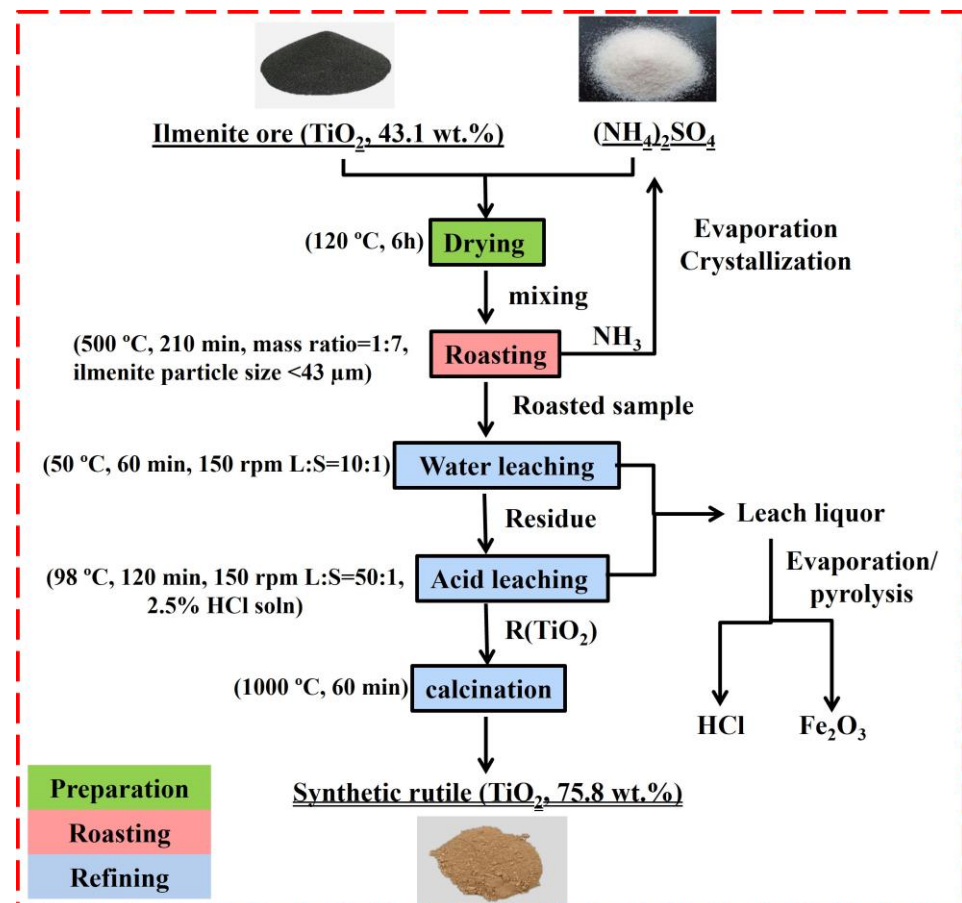


Figure 13. Process flowsheet for the production of TiO_2 from ilmenite via the ammonium sulfate roasting-leaching process.

4. Conclusions

- The recovery of TiO_2 from titanium ores such as ilmenite via traditional methods like smelting or acid leaching processes has disadvantages. These disadvantages include high energy consumption, CO_2 emissions, and acid waste emissions. Therefore, there is an urgent need for an efficient, economical, clean, and sustainable technology for the recovery of TiO_2 from ilmenite ore.
- An ammonium sulfate roasting method was proven to be an effective way to convert metal oxides in ilmenite ore to soluble sulfates at a low temperature. $(\text{NH}_4)_2\text{SO}_4$ acted as a sulfation agent to produce $\text{NH}_4\text{Fe}(\text{SO}_4)_2$, $\text{Fe}_2(\text{SO}_4)_3$, TiOSO_4 , and Fe_2O_3 during

the roasting process. The roasted products were leached by water, followed by diluted HCl acid.

- The optimal iron leaching efficiency was 49.6% at the following roasting conditions: roasting temperature of 500 °C, roasting time of 210 min, ilmenite-to-(NH₄)₂SO₄ mass ratio of 1:7, and ilmenite particle size of less than 43 μm. The second-stage roasting enhanced the iron leaching efficiency from 49.6% to 53.3%.
- The obtained synthetic rutile after calcination had a TiO₂ grade of 75.83 wt.%. According to the XRD analysis, the main phase was rutile-TiO₂, with small diffraction peaks of Fe₂TiO₅. The iron removal efficiency was not high due to the non-sulfated ilmenite particles shown in the XRD and SEM-EDS analysis. These remaining non-sulfated ilmenite particles, which were surrounded by a metal sulfate layer, demonstrate the complexity of the ilmenite ore crystal structure. Therefore, more attention should be paid to the crystal structure breakdown of ilmenite in future studies.
- During this process, ammonium sulfate and hydrochloric acid can be recycled, as well as iron that is wasted in the solution. Therefore, the process is environmentally friendly.

Author Contributions: Conceptualization, L.X. and M.S.A.; methodology, M.S.A., K.E.-B., Y.G. and L.X.; investigation, M.S.A.; software, M.S.A. and Y.G.; writing—original draft, M.S.A.; resources, K.E.-B., Y.G. and L.X.; review and editing, L.X. and M.S.A.; supervision, L.X. and K.E.-B.; funding acquisition, L.X. All authors have read and agreed to the published version of the manuscript.

Funding: The research was funded by the Science and Technology Innovation Program of Hunan Province (Hejian Project No. 2022RC1084) and the “111” project (Green and Value-Added Metallurgy of Non-ferrous Resources). The first author is also grateful for the financial support from the Chinese Scholarship Council.

Data Availability Statement: Not applicable.

Conflicts of Interest: The authors declare no conflict of interest.

References

1. Diebold, U. The Surface Science of Titanium Dioxide. *Surf. Sci. Rep.* **2003**, *48*, 53–229. [\[CrossRef\]](#)
2. Chen, G.; Peng, J.H.; Chen, J. Optimizing Conditions for Wet Grinding of Synthetic Rutile Using Response Surface Methodology. *Min. Metall. Explor.* **2011**, *28*, 44–48. [\[CrossRef\]](#)
3. Awwad, N.S.; Ibrahim, H.A. Kinetic Extraction of Titanium (IV) from Chloride Solution Containing Fe (III), Cr (III) and V (V) Using the Single Drop Technique. *J. Environ. Chem. Eng.* **2013**, *1*, 65–72. [\[CrossRef\]](#)
4. Huang, Y.; Chai, W.; Han, G.; Wang, W.; Yang, S.; Liu, J. A Perspective of Stepwise Utilisation of Bayer Red Mud: Step Two—Extracting and Recovering Ti from Ti-Enriched Tailing with Acid Leaching and Precipitate Flotation. *J. Hazard. Mater.* **2016**, *307*, 318–327. [\[CrossRef\]](#) [\[PubMed\]](#)
5. Zhang, L.; Zhang, J.H.; Zhang, W.; Li, G.Q. Thermodynamic Analysis of Extraction of Synthetic Rutile from Modified Slag. *Ind. Eng. Chem. Res.* **2013**, *52*, 4924–4931. [\[CrossRef\]](#)
6. Froes, F. *Titanium: Physical Metallurgy, Processing, and Applications*; ASM International: Novelt, OH, USA, 2015; ISBN 1627080805.
7. Li, C.; Liang, B. Study on the Mechanochemical Oxidation of Ilmenite. *J. Alloys Compd.* **2008**, *459*, 354–361. [\[CrossRef\]](#)
8. Ellsworth, D.K.; Verhulst, D.; Spitler, T.M.; Sabacky, B.J. Titanium Nanoparticles Move to the Marketplace. *Chem. Innov.* **2000**, psd
9. *Mineral Commodity Summaries 2023*; ASM International: Reston, VA, USA, 2023. [\[CrossRef\]](#)
10. Kahn, J.A. Non-Rutile Feedstocks for the Production of Titanium. *JOM* **1984**, *36*, 33–38. [\[CrossRef\]](#)
11. Itoh, S.; Sato, S.; Ono, J.; Okada, H.; Nagasaka, T. Feasibility Study of the New Rutile Extraction Process from Natural Ilmenite Ore Based on the Oxidation Reaction. *Metall. Mater. Trans. B* **2006**, *37*, 979–985. [\[CrossRef\]](#)
12. El-Hazek, N.; Lasheen, T.A.; El-Sheikh, R.; Zaki, S.A. Hydrometallurgical Criteria for TiO₂ Leaching from Rosetta Ilmenite by Hydrochloric Acid. *Hydrometallurgy* **2007**, *87*, 45–50. [\[CrossRef\]](#)
13. Samal, S.; Mohapatra, B.K.; Mukherjee, P.S.; Chatterjee, S.K. Integrated XRD, EPMA and XRF Study of Ilmenite and Titania Slag Used in Pigment Production. *J. Alloys Compd.* **2009**, *474*, 484–489. [\[CrossRef\]](#)
14. Hamor, L. Titanium Dioxide Manufacture, a World Source of Ilmenite, Rutile, Monazite and Zircon. In *Conference Proceedings*; AusIMM: Perth, WA, USA, 1986; pp. 143–146.
15. Nafziger, R.H.; Elger, G.W. *Preparation of Titanium Feedstock from Minnesota Ilmenite by Smelting and Sulfation-Leaching*; US Department of the Interior, Bureau of Mines: Washington, DC, USA, 1987.
16. Zhang, X.; Du, Z.; Zhu, Q.; Li, J.; Xie, Z. Enhanced Reduction of Ilmenite Ore by Pre-Oxidation in the View of Pore Formation. *Powder Technol.* **2022**, *405*, 117539. [\[CrossRef\]](#)

17. Jia, L.; Liang, B.; Lü, L.; Yuan, S.; Zheng, L.; Wang, X.; Li, C. Beneficiation of Titania by Sulfuric Acid Pressure Leaching of Panzhihua Ilmenite. *Hydrometallurgy* **2014**, *150*, 92–98. [[CrossRef](#)]
18. Middlemas, S.; Fang, Z.Z.; Fan, P. A New Method for Production of Titanium Dioxide Pigment. *Hydrometallurgy* **2013**, *131*, 107–113. [[CrossRef](#)]
19. Zhang, L.; Hu, H.; Liao, Z.; Chen, Q.; Tan, J. Hydrochloric Acid Leaching Behavior of Different Treated Panxi Ilmenite Concentrations. *Hydrometallurgy* **2011**, *107*, 40–47. [[CrossRef](#)]
20. Zhang, S.; Nicol, M.J. An Electrochemical Study of the Reduction and Dissolution of Ilmenite in Sulfuric Acid Solutions. *Hydrometallurgy* **2009**, *97*, 146–152. [[CrossRef](#)]
21. Guo, Y.; Liu, S.; Jiang, T.; Qiu, G.; Chen, F. A Process for Producing Synthetic Rutile from Panzhihua Titanium Slag. *Hydrometallurgy* **2014**, *147*, 134–141. [[CrossRef](#)]
22. Sinha, H.N. *Ilmenite Upgrading by the Murso Process*; TMS Paper NO A 72-32; AIME: New York, NY, USA, 1972; 14p.
23. Robinson, M.; Clamp, F.; Mobbs, D.B.; Pearse, R.V. Laporte High-Efficiency Ilmenite Beneficiation Process. *Proc. Symp. Adv. Extr. Metall.* **1977**, 89–96, 1977.
24. Kataoka, S.; Yamada, S. Acid Leaching Upgrades Ilmenite to Synthetic Rutile. *Chem. Eng.* **1973**, *80*, 92–93.
25. Walpole, E.A.; Winter, J.D. The Austpac ERMS and EARS Processes for the Manufacture of High-Grade Synthetic Rutile by the Hydrochloric Acid Leaching of Ilmenite. In Proceedings of the Chloride Metallurgy 2002-International Conference on the Practice and Theory of Chloride/Metal interaction, Montreal, QC, Canada, 19–23 October 2002.
26. Zhang, W.; Zhu, Z.; Cheng, C.Y. A Literature Review of Titanium Metallurgical Processes. *Hydrometallurgy* **2011**, *108*, 177–188. [[CrossRef](#)]
27. Li, P.; Luo, S.; Wang, X.; Wang, L.; Wang, J.; Teng, F.; Wang, Q.; Zhang, Y.; Liu, X.; Zhang, H. Study on the High-Efficiency Separation of Fe and Mn from Low-Grade Pyrolusite and the Preparation of LiMn₂O₄ Materials for Lithium-Ion Batteries. *Sep. Purif. Technol.* **2021**, *278*, 119611. [[CrossRef](#)]
28. Li, G.; Xiong, X.; Wang, L.; Che, L.; Wei, L.; Cheng, H.; Zou, X.; Xu, Q.; Zhou, Z.; Li, S. Sulfation Roasting of Nickel Oxide–Sulfide Mixed Ore Concentrate in the Presence of Ammonium Sulfate: Experimental and DFT Studies. *Metals* **2019**, *9*, 1256. [[CrossRef](#)]
29. Ju, J.; Feng, Y.; Li, H.; Ma, R.; Wang, B. A Sustainable Low-Temperature Roasting and Water Leaching Process for Simultaneously Extracting Mn, Cu, Co, and Ni from Ocean Manganese Nodules. *J. Sustain. Metall.* **2022**, *8*, 1948–1960. [[CrossRef](#)]
30. Nagaishi, T.; Ishiyama, S.; Matsumoto, M.; Yoshinaga, S. Reactions between Ammonium Sulphate and Metal Oxides (Metal = Cr, Mn and Fe) and Thermal Decomposition of the Products. *J. Therm. Anal.* **1984**, *29*, 121–129. [[CrossRef](#)]
31. Zhang, G.; Luo, D.; Deng, C.; Lv, L.; Liang, B.; Li, C. Simultaneous Extraction of Vanadium and Titanium from Vanadium Slag Using Ammonium Sulfate Roasting-Leaching Process. *J. Alloys Compd.* **2018**, *742*, 504–511. [[CrossRef](#)]
32. Tian, D.; Shen, X.; Zhai, Y.; Xiao, P.; Webley, P. Extraction of Iron and Aluminum from High-Iron Bauxite by Ammonium Sulfate Roasting and Water Leaching. *J. Iron Steel Res. Int.* **2019**, *26*, 578–584. [[CrossRef](#)]
33. Tang, Y.; Zhang, B.; Xie, H.; Qu, X.; Xing, P.; Yin, H. Recovery and Regeneration of Lithium Cobalt Oxide from Spent Lithium-Ion Batteries through a Low-Temperature Ammonium Sulfate Roasting Approach. *J. Power Sources* **2020**, *474*, 228596. [[CrossRef](#)]
34. Deng, L.; Qu, B.; Su, S.-J.; Ding, S.-L.; Sun, W.-Y. Extraction of Iron and Manganese from Pyrolusite Absorption Residue by Ammonium Sulphate Roasting–Leaching Process. *Metals* **2018**, *8*, 38. [[CrossRef](#)]
35. Mu, W.; Cui, F.; Huang, Z.; Zhai, Y.; Xu, Q.; Luo, S. Synchronous Extraction of Nickel and Copper from a Mixed Oxide-Sulfide Nickel Ore in a Low-Temperature Roasting System. *J. Clean. Prod.* **2018**, *177*, 371–377. [[CrossRef](#)]
36. Lee, C.T.; Sohn, H.Y. Recovery of Synthetic Rutile and Iron Oxide from Ilmenite Ore by Sulfation with Ammonium Sulfate. *Ind. Eng. Chem. Res.* **1989**, *28*, 1802–1808. [[CrossRef](#)]
37. Liu, W.; Wang, X.; Lu, Z.; Yue, H.; Liang, B.; Lü, L.; Li, C. Preparation of Synthetic Rutile via Selective Sulfation of Ilmenite with (NH₄)₂SO₄ Followed by Targeted Removal of Impurities. *Chinese J. Chem. Eng.* **2017**, *25*, 821–828. [[CrossRef](#)]
38. Halstead, W.D. Thermal Decomposition of Ammonium Sulphate. *J. Appl. Chem.* **1970**, *20*, 129–132. [[CrossRef](#)]
39. Kiyoura, R.; Urano, K. Mechanism, Kinetics, and Equilibrium of Thermal Decomposition of Ammonium Sulfate. *Ind. Eng. Chem. Process Des. Dev.* **1970**, *9*, 489–494. [[CrossRef](#)]
40. Nakamura, H.; Hara, Y.; Osada, H. The Thermal Decomposition of Ammonium Sulfate and Its Reaction with Iron (III) Oxide. *Nippon Kagaku Kaishi* **1980**, *5*, 706–710. [[CrossRef](#)]
41. Kim, W.-B.; Park, Y.-S.; Lee, C.-T.; Ryoo, Y.-H. Sulfidization of Titaniferous Magnetite with Elemental Sulfur. *Korean Chem. Eng. Res.* **1985**, *23*, 425.

Disclaimer/Publisher’s Note: The statements, opinions and data contained in all publications are solely those of the individual author(s) and contributor(s) and not of MDPI and/or the editor(s). MDPI and/or the editor(s) disclaim responsibility for any injury to people or property resulting from any ideas, methods, instructions or products referred to in the content.